

Supplementary Information

Novel Earth-abundant Cu₃P with TiO₂ Architectured High Efficient “P-N” Heterojunction Nanophotocatalyst for Water Splitting Hydrogen Evolution

Xinzheng Yue^a, Shasha Yi^b, Runwei Wang^a, Zongtao Zhang^{a,*} and Shilun Qiu^a

^aState Key Laboratory of Inorganic Synthesis and Preparative Chemistry, College of Chemistry, Jilin University, Changchun 130012, China.

^bKey Laboratory of Automobile Materials, Ministry of Education, Department of Materials Science and Engineering, Jilin University, Changchun 130022, China.

*Corresponding author: Zongtao Zhang

Tel: +86-431-85168115

Fax: +86-431-85168115

E-mail address: zhang@jlu.edu.cn



Fig. S1 Hydrogen gas evolution equipments.

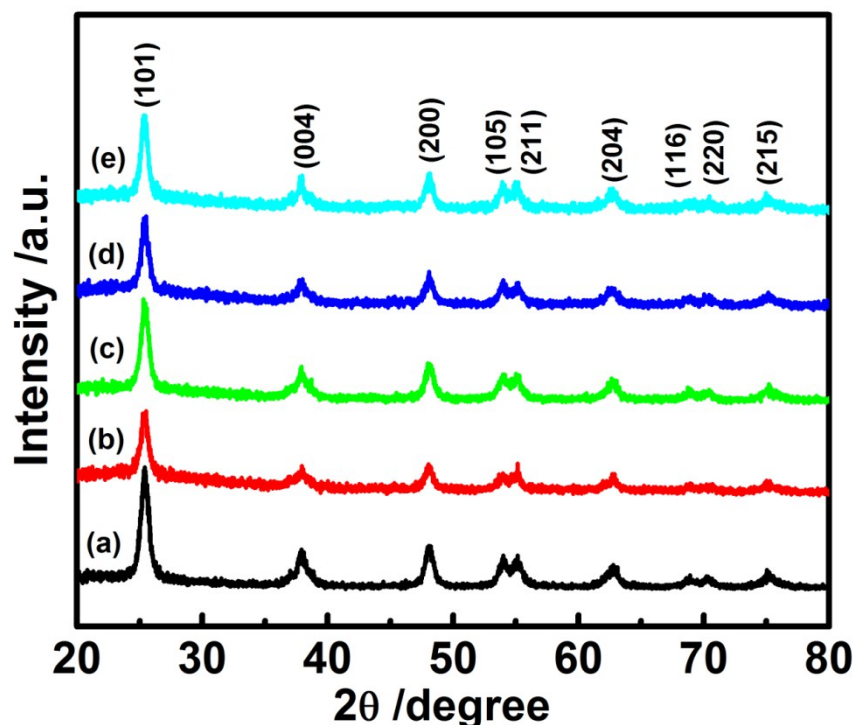


Fig. S2 XRD patterns of the as-prepared $\text{Cu}_3\text{P}/\text{TiO}_2$ samples with varying Cu_3P to $(\text{Cu}_3\text{P} + \text{TiO}_2)$ mass ratio of (a) 0.125 wt%, (b) 0.5 wt%, (c) 1 wt%, (d) 2 wt%, and (e) 5 wt%.

All the peaks observed can be ascribed to the planes of anatase phase TiO_2 (JCPDS-65-5714) and no characteristic diffraction peaks of Cu_3P were observed.

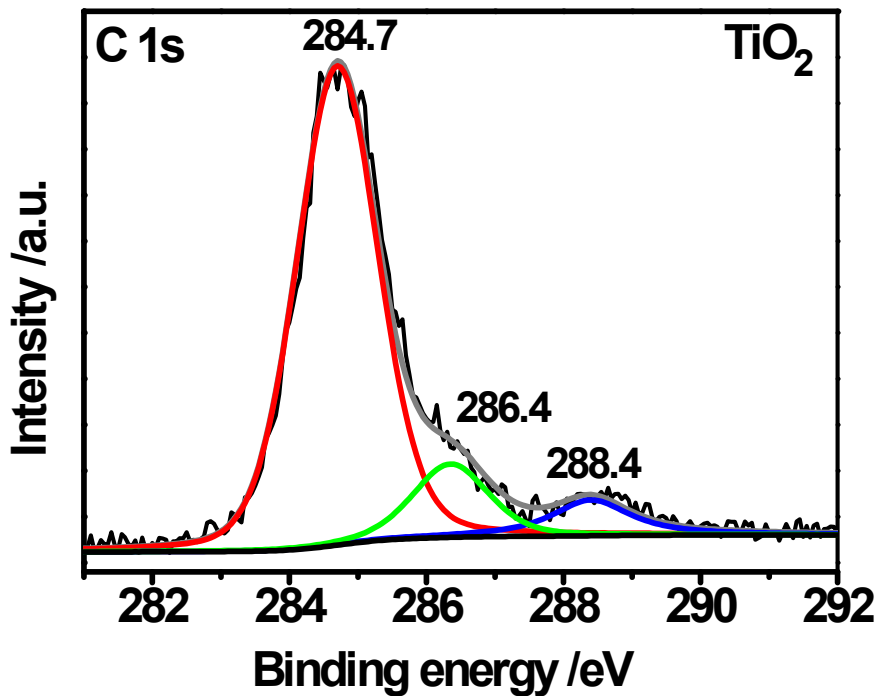


Fig. S3 XPS spectrum of C 1s for TiO_2 sample.

Fig. S3 shows the XPS spectrum of C 1s for pure TiO_2 , the two strong peaks located at 284.7 and 286.4 are characteristic of C-C (mainly the extensively delocalized alternant hydrocarbon) and C-O (the oxygen bound species), respectively. The last peak centered at 288.4 eV can be ascribed to Ti-O-C or O-Ti-C structures, suggesting that the preparation process of TiO_2 leading to the carbon doping into its lattice.^{1,2}

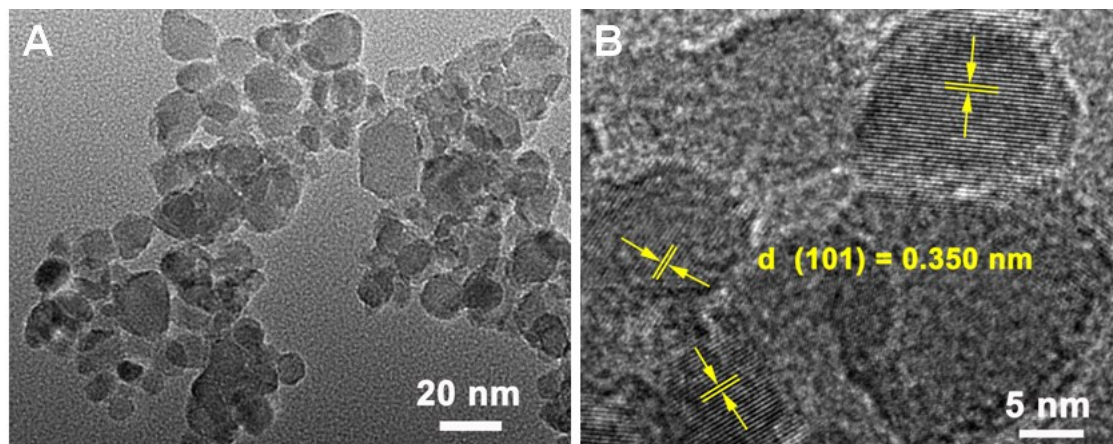


Fig. S4 (A) TEM and (B) HRTEM images of pure TiO_2 product.

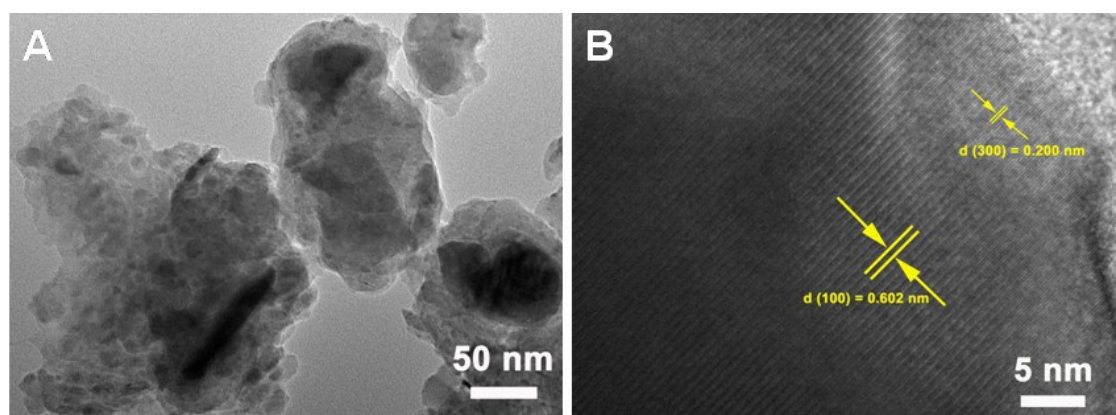


Fig. S5 (A) TEM and (B) HRTEM images of pure Cu_3P product.

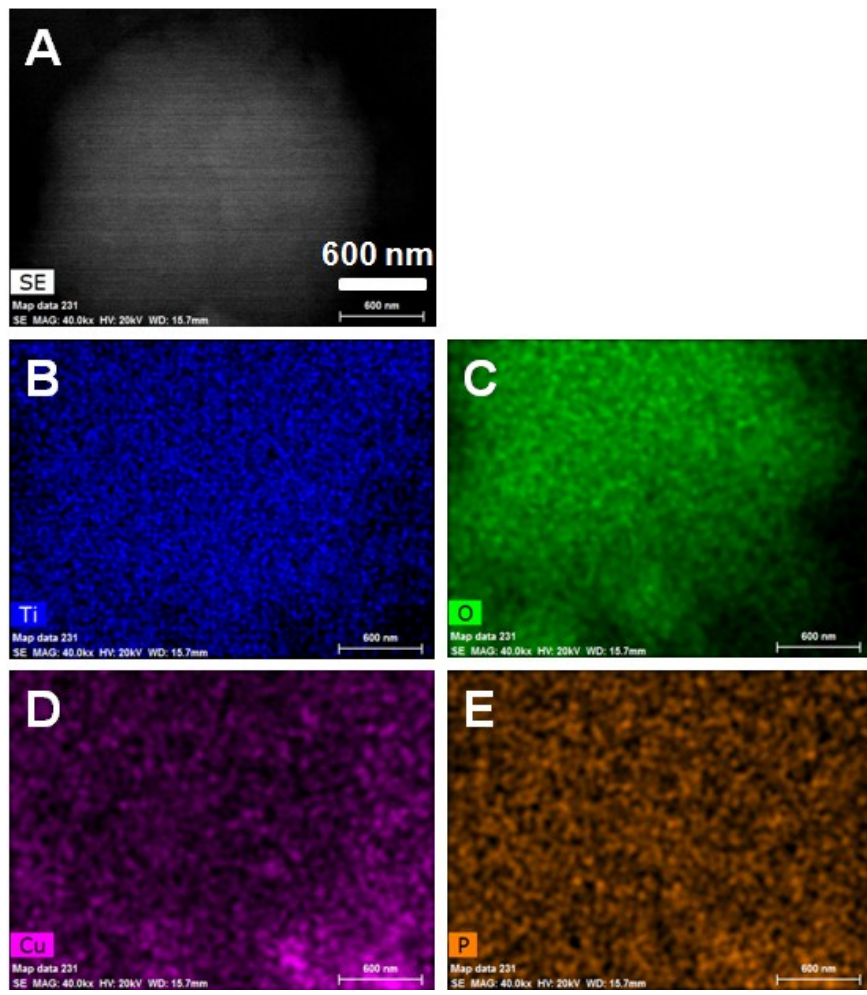


Fig. S6 (A, B-E) Elemental mapping of Ti, O, Cu, and P elements in the 0.5 wt% Cu₃P/TiO₂ product.

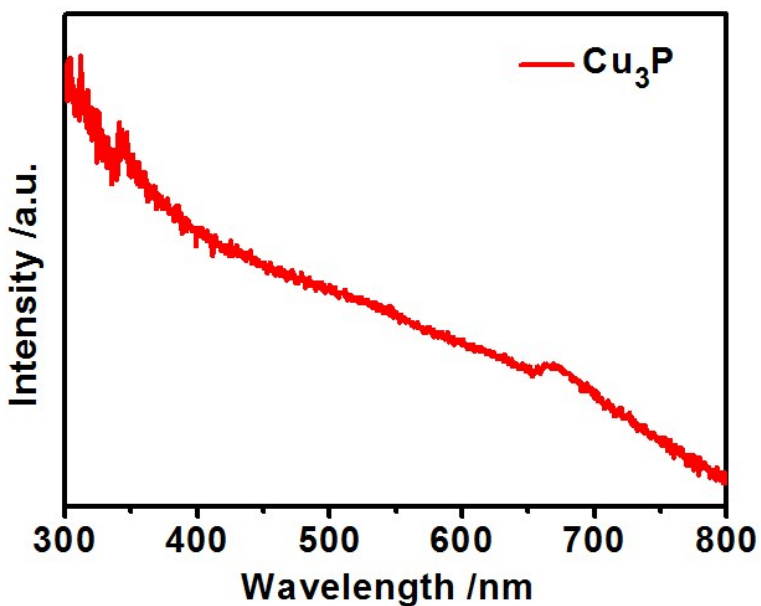


Fig. S7 UV-vis diffuse reflectance spectra (UV-vis DRS) of Cu_3P sample.

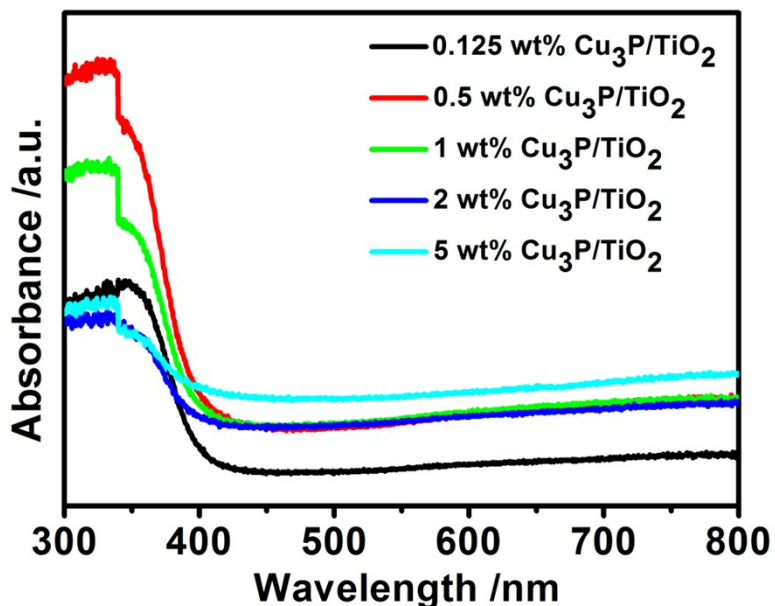


Fig. S8 UV-vis diffuse reflectance spectra (UV-vis DRS) of $\text{Cu}_3\text{P}/\text{TiO}_2$ samples with varying Cu_3P loading.

With the increase of Cu_3P contents in the range from 0.125 to 5%, absorbance intensity of the composite increased in the region of 400-800 nm, meaning its important influence in photocatalytic activity.

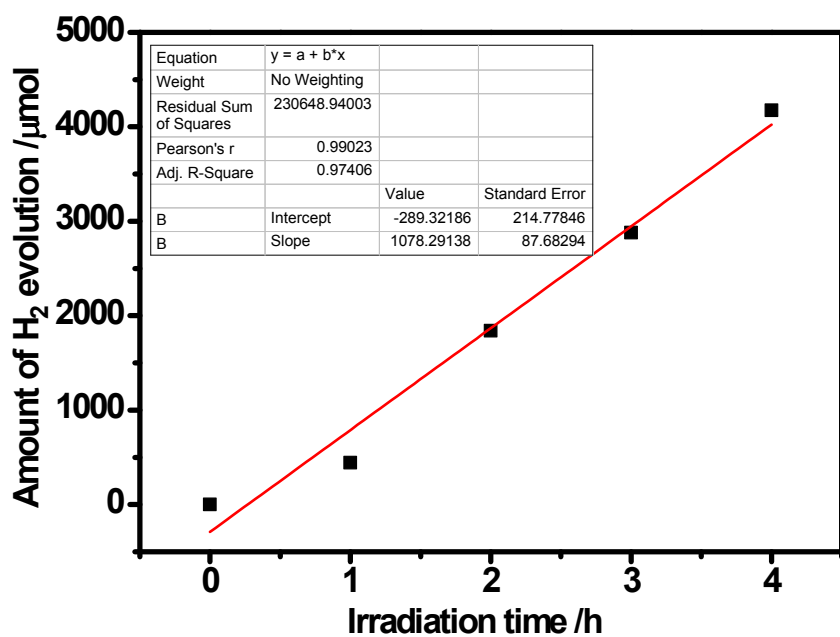


Fig. S9 Photocatalytic H_2 evolution measured for 0.5 wt% $\text{Cu}_3\text{P}/\text{TiO}_2$ at 350 nm in 10 vol% of triethanolamine aqueous solution.

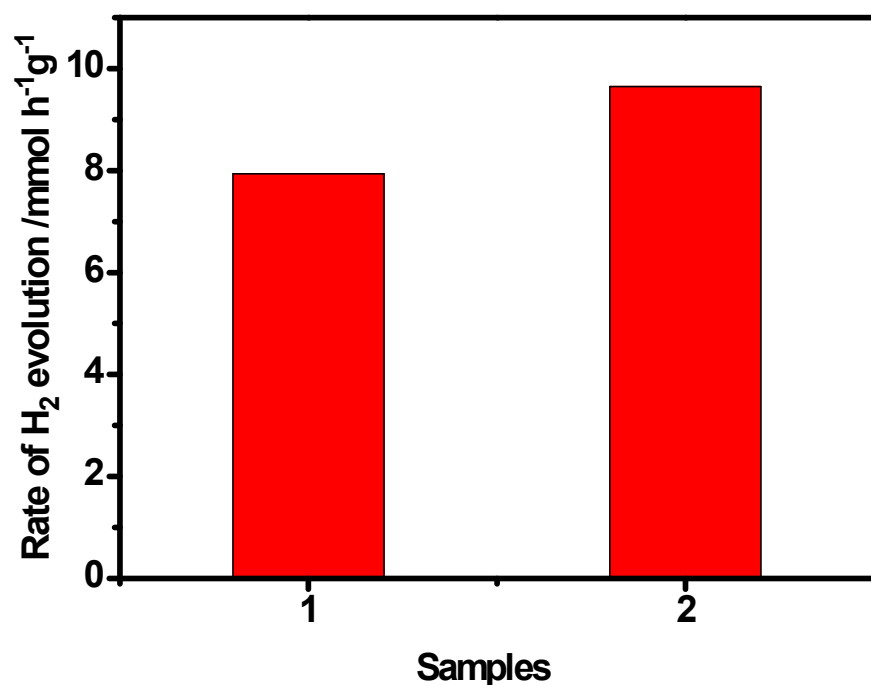


Fig. S10 Comparison of H_2 evolution activities of 0.5 wt% $\text{Cu}_3\text{P}/\text{TiO}_2$ (1) with 0.5wt% Pt/TiO₂ (2).

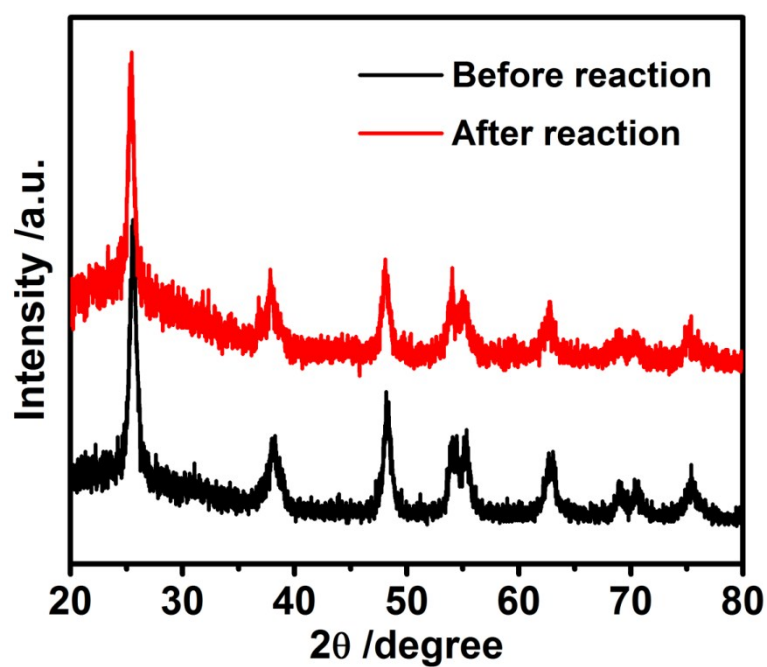


Fig. S11 XRD patterns of 0.5 wt% Cu₃P/TiO₂ before and after the recycling experiments.

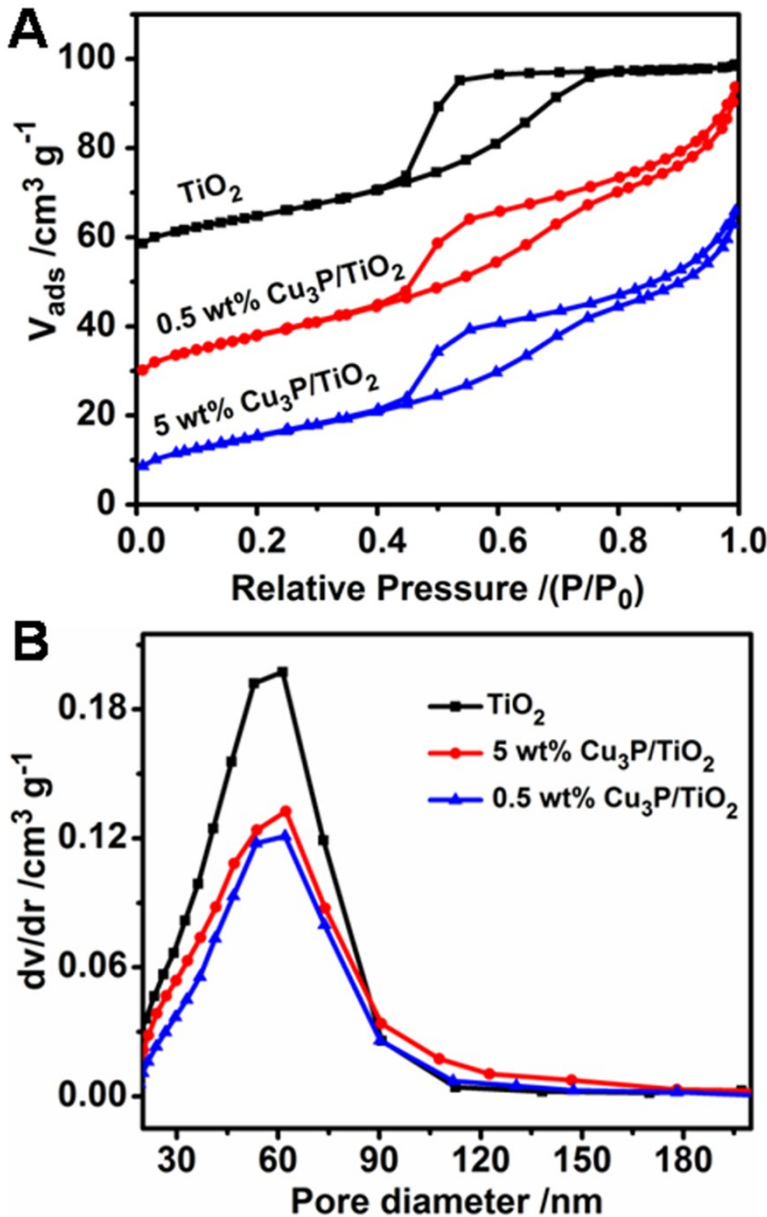


Fig. S12 (A) BET adsorption-desorption isotherms and (B) BJH pore size distribution curves for as-prepared TiO_2 and $\text{Cu}_3\text{P}/\text{TiO}_2$ samples.

The BET surface areas and porous structures of the as-obtained samples were analyzed by performing the nitrogen adsorption-desorption isotherms, shown in Fig. S12. Clearly, the isotherms of all present samples exhibit type V behavior,³ indicating the presence of mesopore may due to the heap up of TiO_2 NCs. The BET surface areas of the TiO_2 ($54.98 \text{ m}^2 \text{ g}^{-1}$), 0.5 wt% $\text{Cu}_3\text{P}/\text{TiO}_2$ ($66.25 \text{ m}^2 \text{ g}^{-1}$), and 5 wt% $\text{Cu}_3\text{P}/\text{TiO}_2$ ($56.71 \text{ m}^2 \text{ g}^{-1}$) samples are slightly higher than that of P25 TiO_2 ($\sim 50 \text{ m}^2 \text{ g}^{-1}$).⁴ Fig. S12 shows the BJH pore size distribution of the samples with the pore

volume of TiO₂, 0.5 wt% Cu₃P/TiO₂, and 5 wt% Cu₃P/TiO₂ are 0.12, 0.13 and 0.20 m³ g⁻¹, corresponding to their average pore diameters are 61.4, 62.3, and 62.1 nm, respectively. The above data illustrate that the distribution of BET surface area, pore volume and pore size were rather narrower, therefore, it is not the main reason for the enhanced photocatalytic H₂-evolution activity.

Table S1. The loading weight percentage of Cu₃P in Cu₃P/TiO₂ hybrid.

	1	2	3	4	5
Theory values	0.125 wt%	0.5 wt%	1 wt%	2 wt%	5 wt%
ICP values	0.092 wt%	0.435 wt%	0.917 wt%	1.916 wt%	4.892wt%

Table S2. Values of calculated E_{CB} and E_{VB} for TiO₂ and Cu₃P.

Semiconductor	E _g (eV)	E _{VB} (eV)	E _{CB} (eV)
TiO ₂	3.18	2.84	-0.34
Cu ₃ P	1.50	2.17	0.67

Table S3. Comparison of photocatalytic hydrogen evolution performances for Cu₃P/TiO₂ system with other promising photocatalysts.

Photocatalyst	Light source	H ₂ (μmol h ⁻¹ g ⁻¹)	Ref.
GO/TiO ₂	300 Hg	1930	ChemSusChem 2014, 7 , 618 ⁵
Cu(OH) ₂ /TiO ₂	UV-LED (365)	3418	Energy Environ. Sci., 2011, 4 , 1364 ⁶
Cu/TiO ₂	UV-LED (365)	5104	Nano Lett. 2015, 15 , 4853 ⁷
Au/B-TiO ₂	300 Xe	2740	ACS Catal. 2014, 4 , 1451 ⁸
Au@TiO ₂ /CdS	300 Xe	1970	ACS Appl. Mater. Interfaces 2013, 5 , 8088 ⁹
MoS ₂ /RGO/TiO ₂	350 Xe	2066	J. Am. Chem. Soc. 2012, 134 , 6575 ¹⁰
Cu ₂ S/TiO ₂	300 Xe	1430	Chem. Commun. 2015, 51 , 13305 ¹¹
CNT/TiO ₂	200 Hg	2940	Appl. Catal. B Environ. 2015, 179 , 574 ¹²
CdS/TiO ₂	AM 1.5G filter	436	J. Phys. Chem. C 2014, 118 , 23627 ¹³
Ni(OH) ₂ /TiO ₂	UV-LED (365)	3056	J. Phys. Chem. C 2011, 115 , 4953 ¹⁴
Graphene/TiO ₂	350 Xe	736	Nanoscale 2011, 3 , 3670 ¹⁵
Cu₃P/TiO₂	300 Xe	7940	This work

References for SI

- 1 Goriparti. S., Miele. E., Prato. M., Scarpellini. A., Marras. S., Monaco. S., Toma. A.,
Messina. G., Alabastri. A., Angelis. F., Manna. L., Capiglia. C. and Zaccaria. R.,

- ACS Appl. Mater. Interfaces, 2015, **7**, 25139-25146.
- 2 Zhang. Y., Zhao. Z., Chen. J., Cheng. L., Chang. J., Sheng.W., Hu. C. and Cao. S., Appl. Catal. B: Environ., 2015, **165**, 715-722.
- 3 Cao. S., Chen. Y., Hou. C., Lu. X. and Fu, W., J. Mater. Chem. A, 2015, **3**, 6096-6101.
- 4 Li. M., Liu. X., Xiong. Y., Bo. X., Zhang. Y., Han. C. and Guo, L., J. Mater. Chem. A, 2015, **3**, 4255-4265.
- 5 Liu. L., Liu. Z., Liu. A., Gu. X., Ge. C., Gao. F. and Dong. L., ChemSusChem, 2014, **7**, 618-626.
- 6 Yu. J. and Ran., J., Energy Environ. Sci., 2011, **4**, 1364-1371.
- 7 Xiao. S., Liu. P., Zhu. W., Li. G., Zhang. D., Li. H., Nano Lett., 2015, **15**, 4853-4858.
- 8 Wang. F., Jiang. Y., Gautam. A., Li. Y. and Amal. R., ACS Catal., 2014, **4**, 1451-1457.
- 9 Fang. J., Xu. L., Zhang. Z., Yuan. Y., Cao. S., Wang. Z., Yin. L., Liao. Y. and Xue. C., ACS Appl. Mater. Interfaces, 2013, **5**, 8088-8092.
- 10 Xiang. Q., Yu. J. and Jaroniec. M., J. Am.Chem. Soc., 2012, **134**, 6575-6578.
- 11 Zhou. Y., Lei. Y.,Wang. D., Chen., C., Peng. Q. and Li. Y., Chem. Commun., 2015, **51**, 13305-13308.
- 12 Moya. A., Cherevan. A., Marchesan. S., Gebhardt. P., Prato. M., Eder. D. and Vilatela. J., Appl. Catal. B: Environ., 2015, **179**, 574-582.
- 13 Lee. S., Lee. K., Kim. W., Lee. S., Shin. D. and Lee. D., J. Phys. Chem. C, 2014, **118**, 23627-23634.

14 Yu. J., Hai. Y. and Cheng. B., J. Phys. Chem. C, 2011, **115**, 4953-4958.

15 Quanjun Xiang. Q., Jiaguo Yu. J. and Jaroniec. M., Nanoscale 2011, **3**, 3670-3678.